Available online at www.sciencedirect.com
SCIENCE DIRECT®
Journal of the European Ceramic Society 25 (2005) 3085–3088
www.elsevier.com/locate/jeurceramsoc

# Infrared and terahertz dielectric spectra of novel $Bi_2O_3$–$Nb_2O_5$ microwave ceramics

P. Samoukhina [a], S. Kamba [a,*], S. Santhi [a], J. Petzelt [a], M. Valant [b], D. Suvorov [b]

[a] *Institute of Physics, Acad. Sci. Czech Rep., Na Slovance 2, 182 21 Praha 8, Czech Republic*
[b] *Advanced Material Department, Jozef Stefan Institute, Jamova 39, 1000 Ljubljana, Slovenia*

Available online 1 April 2005

**Abstract**

Microwave dielectric properties of fluorite-like $(1-x)Bi_2O_3$–$xNb_2O_5$ solid solutions with various $x$ between 0.1 and 0.26 are compared with complex dielectric response in THz and infrared frequency range between 0.1 and 100 THz, which allows the estimation of intrinsic and extrinsic dielectric losses. The best quality sample with the most attractive properties was found for $x = 0.26$ composition with the permittivity of 86, $Qf = 1000$ GHz and $\tau_f = 120$ ppm/K. Our ceramic system exhibits two different crystal structures depending on $Nb_2O_5$ concentration and it is shown how the infrared reflectivity spectra can help to distinguish the structures. $\tau_f$ can be reduced to zero by mixing of Type II and Type III structures.


*Keywords:* Dielectric properties; Spectroscopy; Insulators

## 1. Introduction

Bismuth oxide is strongly polymorphic, α-, β-, γ- and δ-forms are known. The oxygen-deficient fluorite modification of $Bi_2O_3$, the so-called δ-$Bi_2O_3$, is recognized as one of the best high-temperature solid-state oxygen ion conductor. Although the pure phase is stable only in a rather narrow temperature range above 1000 K, the stability range can be significantly broadened even down to room temperature by doping with transition metal oxides such as $Nb_2O_5$, $Ta_2O_5$, etc. or with rare-earth oxides.[1,2] Early investigations of the δ-$Bi_2O_3$ were motivated by that anionic conduction properties, but recently the system has been found as a perspective class of low-temperature cofired ceramics for microwave (MW) applications.[3]

The crystal structure of $Bi_2O_3$–$Nb_2O_5$ system is deduced from fluorite structure of δ-$Bi_2O_3$ (space group $Fm\bar{3}m$, oxygen sites are 75% occupied) and varies with $Nb_2O_5$ concentration, which gives rise to four different phases.[4–7] Substitution of $Nb^{5+}$ for $Bi^{3+}$ leads to a reduction of the 25% oxygen vacancies found in δ-$Bi_2O_3$. At the same time, the octahedral coordination environment strongly preferred by $Nb^{5+}$ leads to distortion of the cubic fluorite oxygen lattice. The structure can be viewed as incorporation of pyrochlore-type structural motifs (e.g., strings of Nb atoms along $[1\,1\,0]_F$ directions) into the underlying fluorite-type metal atom array.[5] For $x < 0.06$ the δ-$Bi_2O_3$ structure is cubic (Type I) and for $0.06 < x < 0.23$ the structure is pseudocubic (Type II) with incommensurate modulation in all three dimensions ($\delta_i \sim 0.37$).[5] Type II solid-solution represented with $Bi_8Nb_2O_{17}$ was described in details in Ref. [6]. Type III structure (for $x$ near 0.25) was recently analysed in detail and it was shown that it can be refined as $Bi_{94}Nb_{32}O_{221}$ with the space group $I\bar{4}m2$ (#119, $Z = 1$) and it can be described as a hybrid of fluorite and pyrochlore types.[7] Type IV structure can be represented by $Bi_5Nb_3O_{17}$ and it has been shown to be more akin to perovskite-type than to fluoride-type δ-$Bi_2O_3$. Gopalakrishnan et al.[8] proposed a model of Type IV structure based on an intergrowth between $n = 1$ and $n = 2$ members of the perovskite-related Aurivillius family of phases.

Study of the MW dielectric properties of $Bi_2O_3$–$Nb_2O_5$ solid solution showed a continuous increase in permittivity and dielectric losses with increasing concentration of

* Corresponding author. Tel.: +420 2 6605 29 57; fax: +420 2 86890527.
*E-mail address:* kamba@fzu.cz (S. Kamba).

0955-2219/$ – see front matter © 2005 Elsevier Ltd. All rights reserved.
doi:10.1016/j.jeurceramsoc.2005.03.194

$Nb_2O_5$.[3] Temperature coefficient of the resonant frequency was negative throughout the entire range below $x = 0.24$, however, for $x = 0.25$ two structural modifications (Type II and Type III), in dependence of temperature of synthesis, were discovered. Dielectric properties of both phases remarkably differ: pseudocubic Type II has permittivity $\varepsilon' = 100$, quality times frequency factor $Qf = 300$ GHz and temperature coefficient of the resonant frequency $\tau_f = -200$ ppm/K while tetragonal Type III has $\varepsilon' = 90$, $Qf = 750$ GHz and $\tau_f = +100$ ppm/K.

The aim of this contribution is to study the same ceramic samples as in Ref. [3] (i.e. $(1-x)Bi_2O_3$–$xNb_2O_5$ ceramics with $0.1 < x < 0.26$) in the THz and infrared (IR) frequency range for the estimation of intrinsic and extrinsic losses. Namely, THz spectra are mainly sensitive on intrinsic contributions to the complex permittivity and THz dielectric losses can be linearly extrapolated down to MW range to estimate the intrinsic MW losses.[9,10]

## 2. Experimental

The synthesis of the $(1-x)Bi_2O_3$–$xNb_2O_5$ solid solutions in the range of $0.10 < x < 0.26$ were conducted using solid state reaction techniques. Details were published in Ref. [3] together with the radio- and MW-dielectric properties and structural investigation by X-ray powder diffraction. Fifteen different ceramic samples differing in the composition or sintering temperature were investigated.

Disc-shaped samples with diameters of 8 mm and thickness 1–2 mm were used for the reflectivity measurement in the IR region. Spectra were obtained at room temperature using a Fourier Transform spectrometer Bruker IFS 113v with pyroelectric deuterated triglycine sulphate detectors in the frequency range of 20–3300 $cm^{-1}$ (0.6–100 THz) with the resolution of 2 $cm^{-1}$. Reflectivity spectra were fitted together with the complex permittivity $\varepsilon^*(\omega)$ spectra in the THz range using a generalized-oscillator model with the factorized form of the complex dielectric function

$$\varepsilon^*(\omega) = \varepsilon'(\omega) - i\varepsilon''(\omega) = \varepsilon_\infty \prod_{j=1}^{n} \frac{\omega_{LOj}^2 - \omega^2 + i\omega\gamma_{LOj}}{\omega_{TOj}^2 - \omega^2 + i\omega\gamma_{TOj}}, \quad (1)$$

where $\varepsilon^*(\omega)$ is related to reflectivity $R(\omega)$ by

$$R(\omega) = \left| \frac{\sqrt{\varepsilon^*(\omega)} - 1}{\sqrt{\varepsilon^*(\omega)} + 1} \right|^2. \quad (2)$$

$\omega_{TOj}$ and $\omega_{LOj}$ are the transverse and longitudinal frequencies of the $j$-th mode, respectively, and $\gamma_{TOj}$ and $\gamma_{LOj}$ are the respective damping constants. The high-frequency permittivity $\varepsilon_\infty$ results from electronic absorption processes at much higher frequencies than phonon frequencies (typically in UV–vis range).

The complex permittivity was directly measured by transmission time-domain THz spectroscopy in the frequency range 3–30 $cm^{-1}$. Thin plane-parallel platelets of 8 mm diameter and 130 μm thickness were used for this purpose. The obtained IR reflectivity spectra were normalized to corresponding THz reflectivity values calculated from the complex permittivity determined from the time-domain THz spectroscopy.

## 3. Result and discussion

FIR reflectivity spectra of five $(1-x)Bi_2O_3$–$xNb_2O_5$ samples are shown in Fig. 1. It can be seen that on increasing concentration damping of the most phonons decreases, which results in sharpening of reflection bands. An abrupt change in the spectra appears between $x = 0.23$ and 0.25. For the samples with $x \geq 0.25$ new modes appear in the spectra giving the evidence of different crystal structure. Ceramics with $x \leq 0.23$ crystallize in the Type II pseudocubic structure represented by the formula $Bi_8Nb_2O_{17}$. Neglecting the incommensurate modulation in this structure, 78 optic modes can be expected in the centre of Brillouin zone. Detailed factor group analysis of the vibrational modes was not possible to perform due to the lack of structural data with the site symmetries of all atoms in the unit cell. Incommensurate modulation of Type II structure should activate further phonon modes from the entire Brillouin zone in IR spectra, but their strengths are expected to be much lower than those of modes from the Brillouin-zone centre[11] and will not be considered in our spectra. Our fit was achieved with only seven highly damped modes, which is much less than expected. Most of the allowed modes are not resolved in the spectra due to their overlapping and/or low intensity. In Type III (tetragonal) structure the unit cell is represented with much larger formula unit $Bi_{94}Nb_{32}O_{221}$, therefore markedly larger number of modes can be expected in the spectra. However, only two new modes appear, which is again much less than expected. The lower damping of the polar modes gives evidence of larger order in the Type III lattice structure.

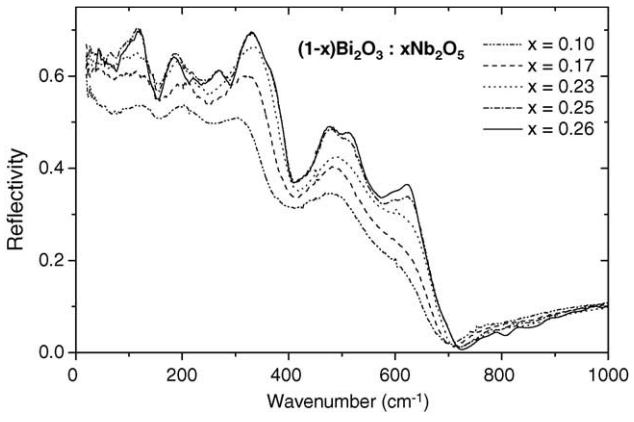


Fig. 1. IR reflectivity spectra of $(1-x)Bi_2O_3$–$xNb_2O_5$ ceramics. All samples were sintered at 900 °C within 3 h.

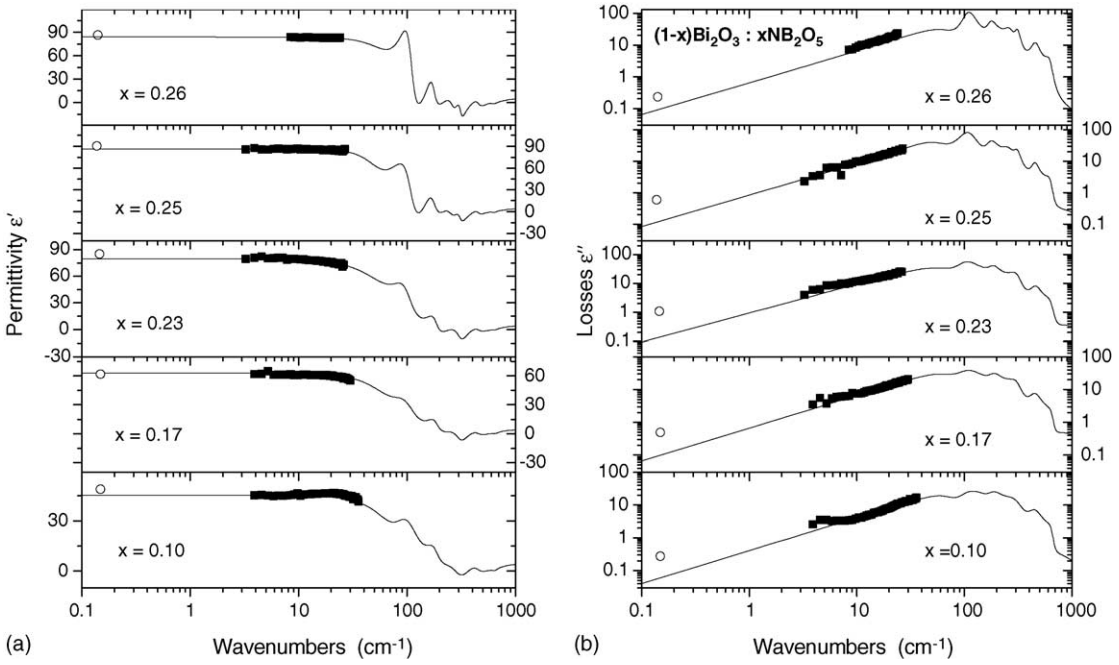


Fig. 2. Real (a) and imaginary (b) part of the complex dielectric function of $(1-x)Bi_2O_3$–$xNb_2O_5$ ceramics calculated from the fits of IR reflectivities and experimental THz data (full symbols). Open symbols show the MW dielectric data from Ref. [3]. Note the change of scale in permittivity for samples with $x \leq 0.17$ and $x \geq 0.23$.

The permittivity $\varepsilon'(\omega)$ and loss $\varepsilon''(\omega)$ spectra obtained from our fits to IR reflectivity are compared with the THz dielectric spectra and the MW data in Fig. 2. One can see that the experimental MW values of $\varepsilon'$ agree very well with the fitted curves. However, higher MW losses were observed in all samples than gives the linear extrapolation from the THz range. The reason for this effect will be discussed below.

A list of all 15 investigated samples is presented in Table 1, where our data are compared with the earlier MW data on the similar samples.[3] MW and THz $\varepsilon'$ are equal within accuracy of the measurements, which gives evidence about no strong dielectric dispersion below the THz region. However, the comparison of the product of quality factor $Q = \varepsilon'/\varepsilon''$ and frequency $f$ obtained from the MW and THz data clearly shows a systematic disagreement. MW $Qf$ values show lower values than $Qf$ obtained from the THz data. It indicates some additional extrinsic MW losses in the samples. Density of all samples was very high and our microstructural study did not observe any defects, so we assume that the losses probably originate from charged point defects. In other words, one could expect that the sample processing could be improved to reach higher $Q$ values. The smallest difference between $Qf$ values in THz and MW experiments (i.e. the smallest extrinsic loss) was observed for the sample with $x = 0.26$. Moreover,

Table 1
List of all investigated $(1-x)Bi_2O_3$–$xNb_2O_5$ ceramics with dielectric data in MW and THz range

| $x$ | $T/t$ | $Qf$ MW (GHz) | $Qf$ THz (GHz) | $\varepsilon'$ MW | $\varepsilon'$ THz | $T$ (ppm/K) |
|---|---|---|---|---|---|---|
| 0.1 | 900 °C/2 h | 797 | 3300 | 49 | 45 | −234 |
| 0.17 | 900 °C/2 h | 559 | 2800 | 62 | 62 | −372 |
| 0.2 | 850 °C/3 h | 430 | 2600 | 79 | 71 | −295 |
| 0.2 | 920 °C/3 h | 421 | 2600 | 80 | 71 | −306 |
| 0.2 | 950 °C/3 h | 405 | 2550 | 77 | 72 | −321 |
| 0.21 | 900 °C/2 h | 382 | 2750 | 77 | 76 | −303 |
| 0.22 | 900 °C/2 h | 370 | 2400 | 84 | 79 | −263 |
| 0.23 | 900 °C/3 h | 346 | 2550 | 85 | 80 | −215 |
| 0.25 | 850 °C/3 h | 725 | 3300 | 92 | 86 | 96 |
| 0.25 | 890 °C/3 h | 674 | 3050 | 91 | 87 | 75 |
| 0.25 | 900 °C/3 h | 630 | 3100 | 90 | 86 | 60 |
| 0.25 | 910 °C/3 h | 526 | 3000 | 93 | 86 | 15 |
| 0.25 | 920 °C/3 h | 334 | 2550 | 95 | 87 | −115 |
| 0.25 | 930 °C/3 h | 309 | 2050 | 98 | 87 | −154 |
| 0.26 | 900 °C/2 h | 996 | 1850 | 86 | 84 | 119 |

Second column characterizes the temperature and duration of sintering.

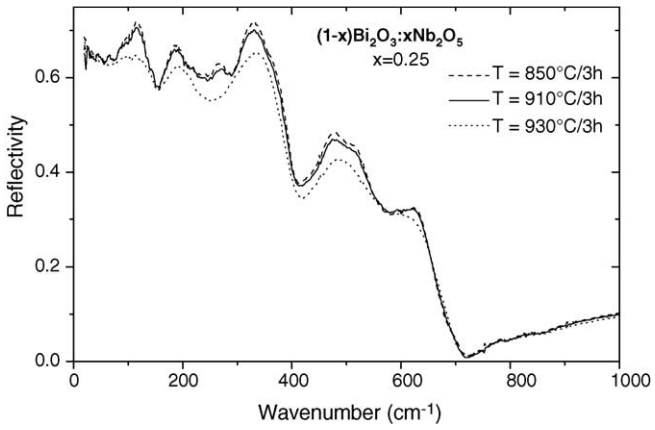


Fig. 3. FIR reflectivity spectra of $0.75Bi_2O_3$–$0.25\,Nb_2O_5$ ceramics sintered at various temperatures.

this sample shows the best value among the studied samples $Qf \cong 1000$ GHz. We cooled the $x = 0.26$ sample down to 20 K and measured the THz dielectric response. Dielectric losses decrease on cooling due to reducing the phonon damping and no evidence of extrinsic contribution to THz losses was observed.

Five $x = 0.25$ samples sintered at different temperatures were studied (see Table 1) and one can see that not only $Qf$ but mainly $\tau_f$ values strongly depend on the sintering conditions. The samples prepared below 910 °C exhibit positive $\tau_f$ while negative $\tau_f$ are seen in samples with higher processing temperature. It is caused by different crystal structure of the samples. Ceramics processed below 910 °C have Type III crystal structure, while the rest of the samples crystallizes in Type II structure.[3] This is manifested also in our IR reflectivity spectra—see Fig. 3. Lower number of phonons and higher damping of the modes is seen in the spectrum of the sample processed at 930 °C (Type II). It is seen in Table 1 that positive $\tau_f$ of samples with $x = 0.25$ decreases with sintering temperature. This means that the samples are not single phase Type III but exhibit small amount of second phase with Type II structure.[3] Finally pure Type II structure with negative $\tau_f$ stabilizes in the sample sintered at 930 K. One can see that most samples have too large $\tau_f$, only the $x = 0.25$ sample sintered at 910 °C has the smallest $\tau_f = 15$ ppm/K and could be used for some MW applications.

## 4. Conclusion

$(1 - x)Bi_2O_3$–$xNb_2O_5$ solid solution was studied using IR and THz spectroscopy. IR reflectivities show different shape of spectra in crystal Type II ($x \leq 0.23$) and Type III ($x \geq 0.25$) ceramics due to different selection rules for phonons in IR spectra. All ceramics show both intrinsic and extrinsic dielectric losses, the sample with $x = 0.26$ is optimised and shows the smallest extrinsic losses. This sample exhibits also highest $Qf$ value of 1000 GHz and simultaneously rather high permittivity ($\varepsilon' = 86$). However, its $\tau_f = 119$ ppm/K is too high for most MW applications. Nevertheless, $\tau_f$ can be reduced by mixing of Type II and Type III structures.

## Acknowledgments

We appreciate support of the Grant Agency of the Czech Republic (project No 202/04/0993), Czech Academy of Sciences (project No A1010213) and Czech Ministry of Education (project COST OC 525.20).

## References

1. Takahashi, T., Iwahara, H. and Esaka, T., High oxide ion conduction in sintered oxide of the system $Bi_2O_3$–$M_2O_5$. *J. Electrochem. Soc.*, 1977, **124**, 1563–1569.
2. Takahashi, T. and Iwahara, H., Oxide ion conductors based on bismuth sesquioxide. *Mater. Res. Bull.*, 1978, **13**, 1447–1453.
3. Valant, M. and Suvorov, D., Dielectric properties of the fluorite-like $Bi_2O_3$–$Nb_2O_5$ solid solution and the tetragonal $Bi_3NbO_7$. *J. Am. Ceram. Soc.*, 2003, **86**, 939–944.
4. Ling, C. D., Withers, R. L., Schmid, S. and Thompson, J. G., A review of bithmuth-rich binary oxides in system $Bi_2O_3$–$Nb_2O_5$, $Bi_2O_3$–$Ta_2O_5$, $Bi_2O_3$–$MoO_3$, and $Bi_2O_3$–$WO_3$. *J. Solid State Chem.*, 1998, **137**, 42–61.
5. Ling, C. D., Structural relationships among bismuth-rich phases in the $Bi_2O_3$–$Nb_2O_5$, $Bi_2O_3$–$Ta_2O_5$, $Bi_2O_3$–$MoO_3$, and $Bi_2O_3$–$WO_3$ systems. *J. Solid State Chem.*, 1999, **148**, 380–405.
6. Withers, R. L., Ling, C. D. and Schmid, S., Atomic modulation functions, periodic nodal surfaces and the three-dimensional incommensurately modulated $(1 - x)Bi_2O_3$–$xNb_2O_5$ $0.06 < x < 0.23$ solid solution. *Z. Kristallogr.*, 1999, **214**, 296–304.
7. Ling, C. D. and Johnson, M., Modeling refinement and analysis of the "Type III" δ-$Bi_2O_3$-related superstructure in the $Bi_2O_3$–$Nb_2O_5$ System. *J. Solid State Chem.*, 2004, **177**, 1838–1846.
8. Gopalakrishnan, J., Ramanan, A., Rao, C. N. R., Jefferson, D. A. and Smith, D. J., A homologous series of recurrent intergrowth structures of the type $Bi_4A_{m+n-2}B_{m+n}O_{3(m+n)+6}$ formed by oxides of the aurivillius family. *J. Solid State Chem.*, 1984, **55**, 101–105.
9. Petzelt, J., Kamba, S., Kozlov, G. V. and Volkov, A. A., Dielectric properties of microwave ceramics investigated by infrared and submillimetre spectroscopy. *Ferroelectrics*, 1996, **176**, 145–165.
10. Petzelt, J. and Kamba, S., Submillimetre and infrared response of microwave materials: extrapolation to microwave properties. *Mater. Chem. Phys.*, 2003, **79**, 175–180.
11. Petzelt, J., Dielectric and light scattering spectroscopy of incommensurate phases in crystals. *Phase Trans.*, 1981, **2**, 155–230.